Detecting Saline Soils with Video Imagery

J. H. Everitt, D. E. Escobar, A. H. Gerbermann, and *M. A. Alaniz*
USDA Agricultural Research Service, Remote Sensing Research Unit, Weslaco, TX 78596

ABSTRACT: A study was conducted in southern Texas to evaluate the potential of using video imagery for distinguishing saline soils in agricultural and rangeland environments. A multi-video imaging system was used to acquire imagery of three areas with saline soils: (1) a native rangeland area, (2) a pasture, and (3) a dryland farming area. The video system provided immediately useful narrowband black-and-white and color-infrared imagery. Results showed that red narrowband (0.644 to 0.656 μm) black-and-white and color-infrared video imagery were best for distinguishing saline soil areas at all study sites. Moreover, computer-based image analysis of the video images resulted in generally satisfactory identification of saline areas. This technique can permit "percent land area" estimates of soil salinity.

INTRODUCTION

MANY ARID AREA SOILS are affected by high water tables and resultant soil salinity (Myers *et al.*, 1963). These areas occur in both agricultural and rangeland environments (Carter, 1975). Detecting these areas is important to personnel involved in using and managing these soils.

Remote sensing techniques have proven useful for detecting and mapping saline soils. Several investigators have shown that saline soils can be delineated in agricultural and rangeland environments using both aerial photography (Myers *et al.*, 1963, 1966; Colwell, 1974; Everitt *et al.*, 1977; Myers *et al.*, 1983) and satellite imagery (Colwell, 1974; Richardson *et al.*, 1976; Everitt *et al.*, 1981; Myers *et al.*, 1983).

Within the past few years, interest in the application of video imagery to remote sensing has greatly increased. Several studies have shown that video imagery can be used to successfully characterize a variety of agricultural, forest, and rangeland resources (Edwards, 1982; Manzer and Cooper, 1982; Vlcek, 1983; Escobar *et al.*, 1983; Edwards *et al.*, 1984; Meisner and Lindstrom, 1985; Nixon *et al.*, 1985; Everitt and Nixon, 1985). The objective of this study was to evaluate video imagery for detecting saline soils in agricultural and rangeland areas of south Texas.

MATERIALS AND METHODS

Study sites were located in the Lower Rio Grande Valley in extreme southern Texas. Three sites were selected for remote sensing investigations in December 1985 and May 1986. The first experimental site was a rangeland area near Roma, Texas. The area has a diversity of inherently saline and nonsaline soils (Fanning *et al.*, 1965; Thompson *et al.*, 1972; Everitt *et al.*, 1977). Everitt *et al.* (1977) characterized the soils and vegetation of this area and used SKYLAB photography to distinguish between saline and nonsaline rangelands along a 24-km flight line. This same area was used in this study.

The second site was a 20-ha pasture near Mercedes, Texas that was severely effected by salinity. The pasture was seeded to bermudagrass (*Cynodon dactylon*), but was infested with honey mesquite (*Prosopis glandulosa*) and huisache (*Acacia farnesiana*) trees. Soils were made up of Hidalgo sandy clay loam and Raymondville clay loam (Jacobs, 1981).

A third experimental site was located in a dryland farming area near San Perlita, Texas. The area was planted to cotton (*Gossypium hirsutum*) and grain sorghum (*Sorghum bicolor*). Soils of this area are affected by a seasonally high water table and resultant salinity. This area is dominated by sandy clay loam soils primarily of the Hidalgo, Lyford, and Racombes series (Turner, 1982). Myers *et al.* (1963, 1966) described the soils of this area and used aerial photography to distinguish saline from nonsaline soils. Two 5-km flight lines were used as test sites.

A general description of the soils at each study area is given in Table 1.

Imagery of the experimental sites was taken with a multi-video color imaging system comprised of three black-and-white video cameras (1.0-inch tubes) and an equipment rack system which generated the camera's power and color composite imagery (Nixon *et al.*, 1987). The imaging system consisted of two visible (0.4 to 0.7 μm) sensitive cameras and one visible/infrared (0.4 to 1.5 μm) sensitive camera. The equipment rack consisted of a color encoder, a time-date generator, a color sync generator, a pulse distribution amplifier, and a power supply. Visible and near-infrared filters were placed on the camera lenses, giving the system the capability to record selected wavelengths in the visible/near-infrared light region. Red (0.644 to 0.656 μm) and green (0.516 to 0.524 μm) filters were used on the visible sensitive cameras while a near-infrared (0.815 to 0.827 μm) filter was used on the visible/infrared sensitive camera. All the camera zoom lenses were set at 18-mm focal length.

Near-infrared, red, and green black-and-white narrowband video images of the pasture and dryland farming areas and a red narrowband image of the rangeland site were digitized using a I²S* model 70-F image processor interfaced to a Hewlett Packard 1000 model 65 computer. Images of the dryland farming area and rangeland site represented only a portion of these study areas, while that of the pasture depicted most of the study area. Images were entered into the image processor using a Sony Betamax Model SLO-383 video cassette recorder/player and Edutron Model CCD2H-3 time base corrector interfaced to the image processor. Color-infrared composites were made of the pasture and dryland farming areas from three narrowband images of each area. The image processor was used to register the three digitized narrowband images of each area and the color-infrared composites were prepared using the red, green, and blue color channels. Images shown herein were photographed from the display monitor. Digitized images were used for illustration because they had less distortion and were sharper than the analog images. Due to malfunction of the I²S image processing software, however, images could not be analyzed with this system. Consequently, the scenes of each study area were photographed off the display monitor. Two prints were made of each study site. A "mask" was made of one of the prints of each site by tracing areas where saline soils were thought to occur onto a transparent paper overlay of the print. These areas were coded black while the remainder of the mask was left white. The other print of each area was nonmasked. Both

*Trade names are included for the benefit of the reader and do not imply an endorsement of or a preference for the product listed by the U.S. Department of Agriculture.

PHOTOGRAMMETRIC ENGINEERING AND REMOTE SENSING,
Vol. 54, No. 9, September, 1988, pp. 1283–1287.

0099-1112/88/5409–1283$02.25/0

TABLE 1. DESCRIPTION AND ELECTRICAL CONDUCTIVITY (ECe) OF THE SOILS OF THE RANGELAND, PASTURE, AND DRYLAND FARMING AREA STUDY SITES.

Study Site and Soil Series	Texture of surface	Color of Surface[1]	ECe (mmhos/cm)	Taxonomic Class
Rangeland				
Catarina - S[2]	clay	2.5Y 6/2	9.4[5]	Hyperthermic Paleustollic Torrerts
Copita - NS[3]	fine sandy loam	10YR 6/2	0.6[5]	Hyperthermic Ustollic Calciorthids
Garceno - NS	clay loam	10YR 6/3	0.9[5]	Hyperthermic Ustollic Camborthids
Maverick - S	clay	2.5Y 5/4	6.4[5]	Hyperthermic Ustollic Camborthids
Montell - S	clay	10YR 5/1	12.6[5]	Hyperthermic Entic Pellusterts
Ramadero - NS	sandy clay loam	10YR 4/2	0.6[5]	Hyperthermic Cumulic Haplustolls
Zapata - NS	loam	10YR 6/2	0.6[5]	Hyperthermic Ustollic Paleorthids
Pasture				
Hidalgo[4] - S	sandy clay loam	10YR 4/2	28.0	Hyperthermic Typic Calciustolls
Raymondville - NS	clay loam	10YR 5/1	3.0	Hyperthermic Vertic Calciustolls
Dryland farming area				
Hidalgo[4] - NS	sandy clay loam	10YR 4/2	1.5[6]	Hyperthermic Typic Calciustolls
Hidalgo[4] - S	sandy clay loam	10YR 4/2	13.4[7]	Hyperthermic Typic Calciustolls
Lyford - NS	sandy clay loam	10YR 4/2	1.5[6]	Hyperthermic Aquic Haplustalfs
Racombes - S	sandy clay loam	10YR 4/1	13.4[7]	Hyperthermic Pachic Argiustolls

[1]According to *Munsell Book of Color*, Munsell Color Co. Inc., Baltimore, Maryland.
[2]S = Saline
[3]NS = Nonsaline
[4]Hidalgo Series has both saline and nonsaline phases.
[5]ECe values are according to Everitt *et al.* (1977).
[6]Mean ECe value for nonsaline phase of Hidalgo and Lyford series.
[7]Mean ECe value for saline phase of Hidalgo and Racombes series.

masked and nonmasked prints were digitized with an image processing system that consisted of a PC-AT clone computer having a Matrox MVP/AT board and IMAGE-PRO II processing software. Images were subjected to the "index replacement" function which permitted the selection of pixels that represented the saline areas in the scenes. This technique permitted the computer to produce a binary image that delineated the saline areas as black colored pixels and nonsaline areas as white colored pixels. The IMAGE-PRO II "analysis" functions were used to determine the percentage of saline areas in each image.

Ground data were obtained at each study site at the time imagery was taken. Ground photographs were taken to help interpret video images, and observational data were recorded relative to plant species, density, and cover. Soil samples were taken at the Mercedes and San Perlita sites to determine degree of salinity. Sampling sites were chosen by visual selection from areas thought to be saline and nonsaline. Samples were collected from four saline and four nonsaline locations at the Mercedes site and from 20 locations (ten saline and ten nonsaline) at the San Perlita site. Soil samples were taken at depth increments of 0 to 15 cm, 15 to 30 cm, and 30 to 60 cm. The samples were analyzed for electrical conductivity of the saturated extract (ECe) using the method of Richards (1954). ECe data herein represent a mean for the 0 to 60 cm depth increment.

Field reflectance measurements were made on both saline and nonsaline phases of the Hidalgo soil series near Mercedes using a Exotech Model 20 spectroradiometer (Leamer *et al.*, 1973). Reflectance measurements were made on ten randomly selected samples of each soil phase in areas devoid of vegetation. Reflected radiation was measured at 0.05-μm increments over the 0.45 to 0.90 μm region with a sensor that had a 15-degree field-of-view. Reflectance measurements were made at 2.0 m above each soil under clear and sunny conditions between 1100 and 1400 hours. The t-test was used to test mean differences statistically between soil reflectances (Steel and Torrie, 1980). The mean reflectance was calculated from the ten 0.05-μm increments over 0.45 to 0.90 μm region.

RESULTS AND DISCUSSION

The mean ECe values of the soil extracts from the different soil types at each study area are given in Table 1. The ECe values, as related to plant growth by the U.S. Salinity Laboratory staff (Richards, 1954), are as follows: above 4.0 mmhos/cm limits production of most forage crops; above 8.0 mmhos/cm, only moderately salt-tolerant species grow well; and above 12.0 mmhos/cm, only the most salt-tolerant species survive. Based on these guidelines, three soils (Catarina, Montell, and Maverick) in the rangeland area were moderate to highly saline and four were nonsaline. At the pasture area, the Hidalgo soils were highly saline and the Raymondville soils were nonsaline. For the dryland farming area, the Racombes and some of the Hidalgo soils were highly saline, whereas the Lyford and the remaining Hidalgo soils were nonsaline. The Hidalgo soil series has both saline and nonsaline phases, with the saline phase occurring in areas with high water tables.

Figure 1 (lower photo) shows the red narrowband video image of a saline rangeland area near Roma, Texas. The saline clay (Montell soils) range sites have a lighter gray to white tone that can be easily separated from the darker tones of the sandy loam (Copita soils) sites. The road on the left side of the image also has a white tone. Other white areas are essentially bare soil areas or "slicks" with surface deposits of sodium and calcium salts (mostly calcium) which severely limit plant growth (Fanning *et al.*, 1965; Everitt *et al.*, 1977). The saline sites could also be distinguished in the green and near-infrared narrowband images (not shown), but they were more clearly delineated in the red image. However, the saline sites could be easily distinguished in the color-infrared video composite image (not shown). Additional saline sites could be easily separated from nonsaline sites on other imagery taken in this area, with the red narrowband and color-infrared composite images being best.

FIG. 1. Red narrowband video image (lower) of a saline rangeland area near Roma, Texas. Computer classified image (upper) of the digitized red narrowband image of the saline rangeland area. Saline areas are coded black, whereas nonsaline areas have a white code.

Figure 1 (upper photo) shows the computer classification of the digitized red narrowband video image (Figure 1 – lower) of the saline rangeland area. Saline areas have a black code, whereas nonsaline areas are coded white. A comparison of the computer classification of the digitized red image to the conventional red image showed that the computer generally delineated the saline areas from the nonsaline areas. The computer estimated that 28.8 percent of the image had saline soils. In contrast, the computer estimated that 30.0 percent of the photointerpreter's overlay map of the image was comprised of saline soils. These differences were thus judged to be minimal. Most of the differences can probably be attributed to the photointerpreters overlay map where subjective boundary lines were drawn due to the grading between saline and nonsaline soils. However, the inability of the computer to separate the roads from the saline soils in the video image also contributed to the differences. These results showed that computer analyses of video images may be a useful technique to determine area estimates of saline soils.

Plate 1 (lower photo) shows the color-infrared video composite image of the pasture near Mercedes, Texas. Saline soil areas are whitish, bermudagrass has a light orange color, huisache is orange-red, and honey mesquite is reddish-brown. The greatest concentration of saline soils are in the upper portion of the image, but some saline areas are in the center. The saline areas could also be easily identified in the green and red narrowband images, but they could not be separated from some of the huisache trees in the near-infrared narrowband image (narrowband images not shown). The computer classification of the color-infrared video composite image of the pasture is shown in Plate 1 (upper photo). Saline soils have a black code, whereas nonsaline soils are coded white. The computer estimated that 18.8 percent of the color-infrared image (Plate 1 – lower photo) was comprised of saline soils compared to a computer estimate of 18.0 percent saline soils for the photointerpreter's overlay map of the image. A comparison of the computer classification to the color-infrared video image of the pasture demonstrated that the computer clearly distinguished the saline from nonsaline areas.

The color-infrared video composite image of a portion of the dryland farming area near San Perlita, Texas is shown in Plate 2 (lower photo). Saline soil and roads are whitish, nonsaline soil has a light gray color, grain sorghum is intermediate to dark magenta, and cotton is light magenta. The saline soil areas could also be easily delineated in the red narrowband video image and most could be distinguished in the green narrowband video image, but they could not be differentiated from some of the grain sorghum in the near-infrared narrowband image (narrowband images not shown). Additional saline soil areas could be distinguished in other color-infrared composite and red narrowband video imagery obtained at other locations in the study area. Plate 2 (upper photo) shows the computer classification of the color-infrared image of the dryland farming area. Saline soil has a black code, whereas nonsaline soil areas have a white code. Visual comparison of the computer classification (Plate 2 – upper photo) to the color-infrared composite image (Plate 2 – lower photo) shows that the computer over classified the saline soil areas. This is apparent in the left hand side of the print where roads were classified as saline areas. The computer also classified some of the nonsaline areas as saline areas within the fields. This is apparent in the lower right hand portion of the composite image where some of the light gray nonsaline bare soil was identified as saline soil. The computer estimated that 7.0 percent of the color-infrared video image was comprised of saline soils, while it estimated that 4.0 percent of the photointerpreter's overlay map of the image was made up of saline soils. Although the photointerpretation technique also has discrepancy, it was more accurate in this instance.

The ability to distinguish between saline and nonsaline soils in video imagery obtained at all three study areas was primarily attributed to less plant cover on the saline soils. Differentiation between saline and nonsaline soils was also attributed to differences in their soil surface conditions. The saline soils had crusted surfaces that were smoother than the generally rough surfaces of the nonsaline soils, which resulted in saline soils having significantly higher ($p = 0.01$) reflectance than the nonsaline soils over the 0.45 to .90 μm spectral region (Figure 2). Gausman *et al.* (1977) also reported that saline soils had higher visible/near-infrared reflectance than did nonsaline soils. Soil color was deemed to have minimal influence in separating saline from nonsaline soils because of little or no differences in soil color value and soil color chroma among the soils (Table 1). The inability to spectrally separate roads from saline soils was

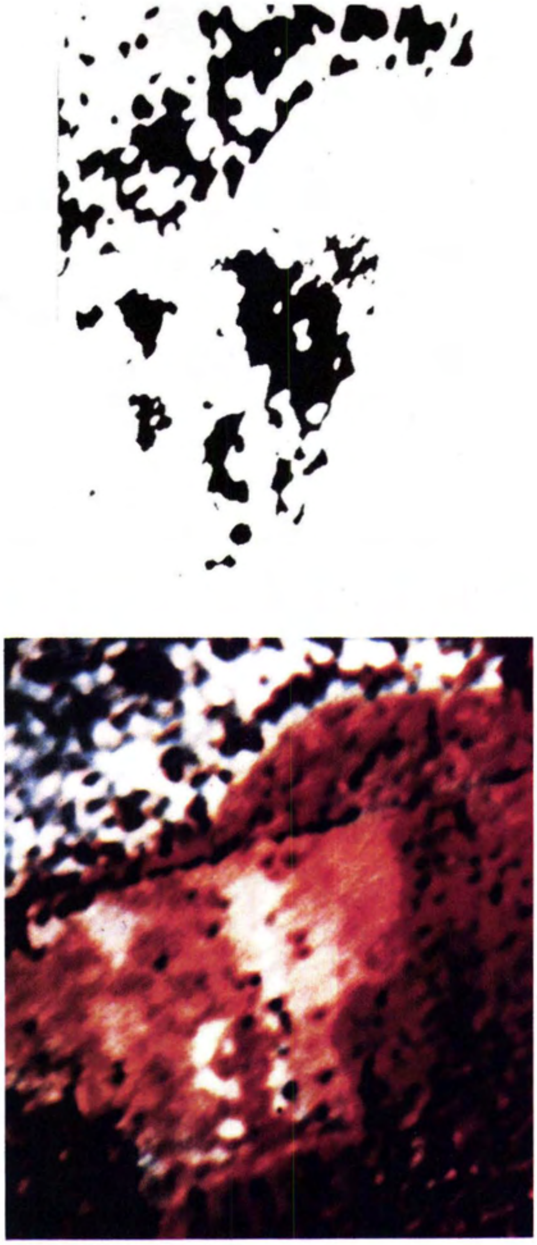

PLATE 1. Color-infrared video composite image (lower) of the pasture near Mercedes, Texas and computer classification (upper) of the composite image. Saline areas are coded black, whereas nonsaline areas have a white code.

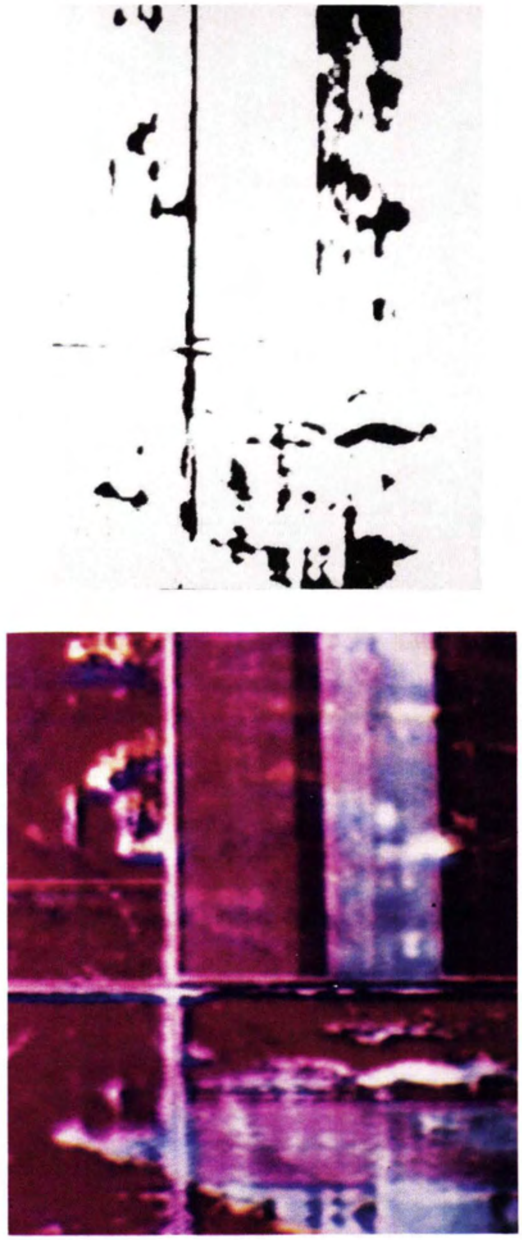

PLATE 2. Color-infrared video composite image (lower) of the dryland farming area near San Perlita, Texas and computer classification (upper) of the composite image. Saline areas are coded black, whereas nonsaline areas have a white code.

attributed to their smooth caliche surfaces which were apparently high in visible/near-infrared reflectance.

CONCLUSIONS

These results showed that video imagery can be used to detect saline soils in both agricultural and rangeland environments in southern Texas. Color-infrared composite and red narrowband video images were superior to green and near-infrared narrowband images for distinguishing areas of soil salinity. The ability to differentiate between saline and nonsaline soils was primarily attributed to less plant cover on the saline soils. But the crusted surfaces of the saline soils also aided in separating them from the nonsaline soils which generally had broken soil surfaces. Computer classification of both color-infrared composite and red narrowband images resulted in generally satisfactory identification of saline soil areas; however, the computer was unable to distinguish between caliche roads and saline soils. The computer analyses can permit area estimates of soil salinity in both agricultural and rangeland areas. These findings should be useful to land-use managers interested in using remote sensing techniques to detect saline soils.

ACKNOWLEDGMENTS

Thanks are extended to Rene Davis for obtaining the video imagery and to Romeo Rodriguez for his assistance in the field and laboratory. The authors also thank Ron Bowen for producing the illustrations and Rick Villarreal for his expertise with image processing.

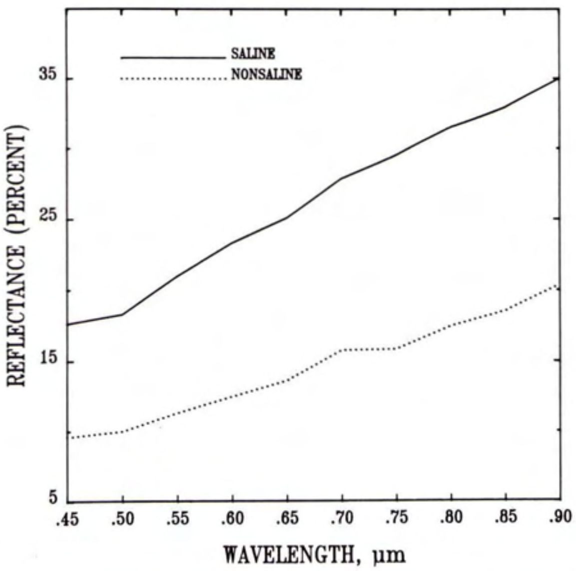

FIG. 2. Field spectroradiometric measured light reflectance over the 0.45 to 0.90 µm spectral region for saline and nonsaline soil.

REFERENCES

Carter, D. L., 1975. Problems of salinity in agriculture. (A. Poljakoff-Mayber and J. Gale, eds.), *Ecological Studies. Analysis and Synthesis, Plants in Saline Environments*. Vol. 15. Springer-Verlag Publishing Company, Berlin, Germany. pp.25–35.

Colwell, R. N., 1974. *An Integrated Study of Earth Resources in the State of California Using Remote Sensing Techniques*. Annual Progress Report, Space Sciences Laboratory, Univ. of Calif. Berkeley. May 1, 1974.

Edwards, G. J., 1982. Near-infrared aerial video evaluation for freeze damage. *Proc. Fla. State Hort. Soc.* 95:1–3.

Edwards, G. J., C. H. Blazquez, K. O'Cuillinn, J. C. McKinnon, C. O. Youtsey, and L. Blesius, 1984. Comparison of aerial color infrared video and 70 mm color infrared photography of citrus trees. *Proc. Fla. State Hort. Soc.* 97:14–16.

Escobar, D. E., R. L. Bowen, H. W. Gausman, and G. R. Cooper, 1983. Use of near-infrared video recording system for the detection of freeze-damaged citrus leaves. *J. Rio Grande Valley Hort. Soc.* 36:61–66.

Everitt, J. H., A. H. Gerbermann, and J. A. Cuellar, 1977. Distinguishing saline from nonsaline rangelands with SKYLAB imagery. *Photogrammetric Engineering and Remote Sensing* 43:1041–1047.

Everitt, J. H., and P. R. Nixon, 1985. Video imagery: A new remote sensing tool for range management. *J. Range Manage.* 38:421–424.

Everitt, J. H., A. J. Richardson, and C. L. Wiegand, 1981. Inventory of semi-arid rangelands in south Texas with LANDSAT data. *Proc. 7th Int. Symp. Machine Processing of Remotely Sensed Data*. Purdue University, West Lafayette, Indiana pp. 404–415.

Fanning, C. D., C. M. Thompson, and D. Isaacs, 1965. Properties of saline soils of the Rio Grande Plain. *J. Range Manage.* 18:190–193.

Gausman, H. W., R. W. Leamer, J. R. Noriega, R. R. Rodriguez, and C. L. Wiegand, 1977. Field-measured spectroradiometric reflectances of disked and nondisked soil with and without straw. *Soil Sci. Soc. Am. J.* 41:793–796.

Jacobs, J. L., 1981. *Soil Survey of Hidalgo County, Texas*. SCS, USDA, Washington, DC. 171 p.

Leamer, R. W., V. I. Myers, and L. F. Silva, 1973. A spectroradiometer for field use. *Rev. Sci. Instrum.* 44:611–614.

Manzer, F. E., and G. R. Cooper, 1982. Use of portable videotaping for aerial infrared detection of potato disease. *Plant Disease* 66:665–667.

Meisner, D. E., and D. M. Lindstrom, 1985. Design and operation of a color infrared aerial video system. *Photogrammetric Engineering and Remote Sensing* 51:555–560.

Myers, V. I., L. R. Ussery, and W. J. Rippert, 1963. Photogrammetry for detailed detection of drainage and salinity problems. *Amer. Soc. Agr. Engr. Trans.* 6:332–334.

Myers, V. I., D. L. Carter, and W. J. Rippert, 1966. Remote sensing for estimating soil salinity. *Amer. Soc. Civ. Engr. J. Irrig. and Drainage* 92, IR 4, Prc. Paper 5040. pp. 59–68.

Myers, V. I., M. E. Bauer, H. W. Gausman, W. G. Hart, J. L. Heilman, R. B. McDonald, A. B. Park, R. A. Ryerson, T. J. Schmugge, and F. C. Westing, 1983. Remote sensing applications in Agriculture. *Manual of Remote Sensing* (Robert N. Colwell, ed.), Amer. Soc. Photogrammetry, Falls Church, Virginia. pp. 2111–2228.

Nixon, P. R., D. E. Escobar, and R. M. Menges, 1985. Use of a multiband video system for quick assessment of vegetal condition and discrimination of plant species. *Remote Sensing of Environment* 17:203–208.

Nixon, P. R., D. E. Escobar, and R. L. Bowen, 1987. A multivideo false color imaging system for remote sensing applications. *Proc. 11th Biennial Workshop on Color Aerial Photography and Videography in the Plant Sciences*. Amer. Soc. Photogrammetry and Remote Sensing, Falls Church, Virginia. pp. 295–305.

Richards, L. A. (ed.), 1954. *Diagnosis and Improvement of Saline and Alkali Soils*. U.S. Dept. Agr. Handbook No. 60. pp. 89–90.

Richardson, A. J., A. H. Gerbermann, H. W. Gausman, and J. A. Cuellar, 1976. Detection of saline soils with SKYLAB multispectral scanner data. *Photogrammetric Engineering and Remote Sensing* 43:679–684.

Steel, R. G. D., and J. H. Torrie, 1980. Principles and procedures of statistics. McGraw-Hill Book Co., Inc., New York. 481 p.

Thompson, C. M., R. S. Sanders, and D. Williams, 1972. *Soil survey of Starr County, Texas*. SCS, USDA, Washington, D.C. 62 p.

Turner, A. J., 1982. *Soil survey of Willacy County, Texas*. SCS, USDA, Washington, D.C. 137 p.

Vlcek, J., 1983. Videography: Some remote sensing applications. *Proc. 49th Annual Meeting Amer. Soc. Photogrammetry*. pp. 63–69.

(Received 9 November 1987; revised and accepted 17 May 1988)

Errata

In our July issue we regret that errors were made in identifying the following individuals:

Page 1031, caption for the Ribbon Cutting: ACSM President Woods's name should be spelled Alberta not Albert.

Page 1049, caption for President's Award for Practical Papers: It is Klaus Szangolies receiving the Deed of Award, not Horst H. Scholer.

Page 1056, list of Past Presidents of ASPRS: Talbert Abrams is the correct spelling, not Abrahams.

Page 1057, caption for President Alden P. Colvocoresses being congratulated by Past-President Graham: Colvocoresses should have a capital C, not a lower case c.

Page 1067, the author's affiliation: Member Emeritus, not Emoritus.